1062 | https://doi.org/10.3311/PPci.14746

Periodica Polytechnica Civil Engineering, 63(4), pp. 1062–1079, 2019

Discrete Sizing of Steel Frames Using Adaptive Dimensional Search Algorithm

Oğuzhan Hasançebi[1], Saeid Kazemzadeh Azad[2*]

[1] Department of Civil Engineering, Faculty of Engineering, Middle East Technical University, Üniversiteler Mahallesi, Dumlupınar Bulvarı, 06800 Çankaya, Ankara, Turkey
[2] Department of Civil Engineering, Faculty of Engineering, Atilim University, Kızılcaşar Mahallesi, 06836 İncek, Ankara, Turkey
* Corresponding author, e-mail: saeid.azad@atilim.edu.tr

Received: 26 July 2019, Accepted: 20 September 2019, Published online: 30 October 2019

Abstract

Adaptive dimensional search (ADS) algorithm is a recently proposed metaheuristic optimization technique for discrete structural optimization problems. In this study, discrete sizing optimization problem of steel frames is tackled using the ADS algorithm. An important feature of the algorithm is that it does not use any metaphor as an underlying principle for its implementation. Instead, the algorithm employs an efficient performance-oriented methodology at each iteration for convergence to the optimum or a near optimum solution. The performance of the ADS is investigated through optimum design of five real-size steel frame structures and the results are compared versus several contemporary metaheuristic techniques. The comparison of the obtained numerical results with those of available designs in the literature reveals the reliability and efficiency of the ADS in optimum design of steel frames.

Keywords

structural design, discrete optimization, steel frames, metaheuristic algorithms, adaptive dimensional search, sizing optimization

1 Introduction

In the last few decades, optimum design of engineering systems received considerable attention in the research community due to the globally increasing economic and environmental concerns. On the one hand, optimization provides the industry with an opportunity to produce more economical designs, and on the other hand, by reducing the material consumption as well as labor hours, alleviates the environmental problems such as carbon footprint of production and construction procedures. In general, optimum design of structural systems requires decision making on a set of design variables with respect to the strength and serviceability requirements imposed by a standard design code. Due to the wide range of applications of steel frames in the construction industry, many research studies addressed methodologies to enhance the design optimization procedure of steel frames so far [1]. Typically, in practical applications the frame members are selected from an available list of steel profiles. Therefore, commonly an optimization problem with discrete design variables is be solved in order to achieve an optimum or a near optimum final design. Indeed, development of numerous discrete optimization methodologies is basically due to the fact that the current computational technologies are not capable of performing an exhaustive search in the solution space by evaluation of all candidate solutions in a timely manner.

In the past decades, various research studies have been conducted on developing efficient design optimization techniques for structural engineering applications [2–9]. In fact, most of the recently proposed optimization algorithms for discrete sizing of steel frames belong to the class of stochastic search techniques or the so-called metaheuristics [2, 10, 11]. In general, metaheuristic techniques, such as genetic algorithms [12], particle swarm optimization [13], ant colony optimization [14, 15], etc., borrow their working principles from natural phenomena [16]; and follow non-deterministic search strategies for locating an optimum or a near optimum solution. The common methodology for development of metaheuristic based structural optimization techniques is to consider the neighborhood of promising candidate solutions found in each iteration to predict the search direction of the next iteration. Usually, a metaheuristic technique performs a global search in the early stages of the optimization, by exploring a wide area of the solution space, and gradually turns into a local

Cite this article as: Hasançebi, O., Kazemzadeh Azad, S. "Discrete Sizing of Steel Frames Using Adaptive Dimensional Search Algorithm", Periodica Polytechnica Civil Engineering, 63(4), pp. 1062–1079, 2019. https://doi.org/10.3311/PPci.14746

search process in the last iterations to enhance the quality of the final solution. The popularity of metaheuristics structural optimization techniques can be attributed to their promising solutions, robust performances, independency to gradient information, and capability of handling both discrete and continuous design variables. The metaheuristic methods of structural optimization as well as their practical applications have been generally surveyed by Lamberti and Pappalettere [17].

For a more efficient search in the design space, adaptive metaheuristics refine their search strategies during the optimization process [18–20]. Recently, an adaptive dimensional search (ADS) technique was proposed by Hasançebi and Kazemzadeh Azad [21] for discrete sizing optimization of truss structures. In the ADS, the search dimensionality ratio (SDR) is adaptively updated, during the optimization process, to control the convergence rate of the algorithm. It was attempted to provide a balance between the exploration and exploitation characteristics of the ADS during its search in the design space based on the performance of the technique at each iteration. The efficiency of the ADS, in discrete truss optimization problems, is demonstrated in Hasançebi and Kazemzadeh Azad [21] compared to several contemporary metaheuristic algorithms. In addition to the efficiency of the ADS in discrete sizing optimization problems, another important feature of the algorithm is that it does not use any metaphor as an underlying principle for its implementation. Instead, the algorithm employs a simple, yet efficient performance-oriented methodology based on the update of the SDR parameter at each iteration for convergence to the optimum or a near optimum solution. This performance-oriented feature of the ADS makes it much easier for structural engineers to better understand the working principles of the technique for coding and implementation.

Considering the promising performance of the ADS in optimum design of truss structures, in the present study, the algorithm is reformulated for tackling discrete sizing optimization problems of real-size steel frames. The performance of the ADS is investigated through optimum design of five real-size steel frame structures, namely a 132-member unbraced space steel frame, a 325-member braced space steel frame, a 568-member unbraced space steel frame, a 744-member unbraced steel frame, and a 1860-member braced steel frame. The results obtained by the ADS demonstrate that the algorithm is capable of locating promising solutions with an acceptable level of conformity to those of other contemporary discrete sizing optimization techniques.

The remaining parts of the study are organized as follows. Section 2 describes the discrete sizing optimization problem of steel frames according to AISC-ASD [22]. In Section 3 provides a detailed description of computational steps involved in the ADS algorithm are overviewed. Section 4 presents the performance evaluation of the ADS algorithm using real-size steel frame instances. Section 5 provides a brief conclusion of the study.

2 Practical design optimization of steel frames

In real-world applications the steel frame members are usually selected from a set of available steel sections, which yields a discrete optimization problem. For a steel frame consisting of N_m members that are collected in N_d member groups, the design optimization problem according to AISC-ASD [22] can be formulated as follows.

The optimization objective is to find a vector of integer values $\mathbf{I}$ (Eq. (1)) representing the sequence numbers of steel sections assigned to N_d member groups,

$$\mathbf{I}^T = \left[I_1, I_2, ..., I_{N_d} \right], \tag{1}$$

to minimize the weight (W) of the frame

$$W = \sum_{i=1}^{N_d} \rho_i A_i \sum_{j=1}^{N_t} L_j \,, \tag{2}$$

where A_i and ρ_i are the length and unit weight of the steel section adopted for member group i, respectively, N_t is the total number of members in group i, and L_j is the length of the member j which belongs to group i.

The frame members subjected to a combination of axial compression and flexural stress should be sized to satisfy the following stress constraints (Eqs. (3)–(5)):

$$if\ \frac{f_a}{F_a} > 0.15;\ \left[\frac{f_a}{F_a} + \frac{C_{mx} f_{bx}}{\left(1 - \frac{f_a}{F'_{ex}}\right) F_{bx}} + \frac{C_{my} f_{by}}{\left(1 - \frac{f_a}{F'_{ey}}\right) F_{by}} \right] - 1.0 \le 0, \tag{3}$$

$$\left[\frac{f_a}{0.60 F_y} + \frac{f_{bx}}{F_{bx}} + \frac{f_{by}}{F_{by}} \right] - 1.0 \le 0 \,, \tag{4}$$

$$if\ \frac{f_a}{F_a} \le 0.15;\ \left[\frac{f_a}{F_a} + \frac{f_{bx}}{F_{bx}} + \frac{f_{by}}{F_{by}} \right] - 1.0 \le 0 \,. \tag{5}$$

If the flexural member is under tension, then the formula given in Eq. (6) is used instead:

$$\left[\frac{f_a}{0.60 F_y} + \frac{f_{bx}}{F_{bx}} + \frac{f_{by}}{F_{by}} \right] - 1.0 \le 0 \,. \tag{6}$$

In Eqs. (3)–(6), F_y is the material yield stress, and $f_a = (P / A)$ represents the calculated axial stress, where A is the cross-sectional area of the member. The calculated flexural stresses due to bending of the member about its major (x) and minor (y) principal axes are denoted by f_{bx} and f_{by}, respectively. F'_{ex} and F'_{ey} denote the Euler stresses about principal axes of the member that are divided by a factory of safety of 23/12. F_a stands for the allowable axial stress under axial compression force alone, and is calculated depending on elastic or inelastic bucking failure mode of the member using Formulas 1.5-1 and 1.5-2 given in AISC-ASD [22]. The allowable bending compressive stresses about major and minor axes are designated by F_{bx} and F_{by}, which are computed using the Formulas 1.5-6a or 1.5-6b and 1.5-7 given in AISC-ASD [22]. It is important to note that while calculating allowable bending stresses, a newer formulation (Eq. (7)) of moment gradient coefficient c_b given in ANSI/AISC 360-05 [23] is employed in the study to account for the effect of moment gradient on lateral torsional buckling resistance of the elements,

$$c_b = \frac{12.5M_{\max}}{2.5M_{\max} + 3M_A + 4M_B + 3M_C} R_m \le 3.0 , \quad (7)$$

where $M_{\max}$, M_A, M_B and M_C are the absolute values of maximum, quarter-point, midpoint, and three-quarter point moments along the unbraced length of the member, respectively, and R_m is a coefficient which is equal to 1.0 for doubly symmetric sections. C_{mx} and C_{my} are the reduction factors, introduced to counterbalance overestimation of the second-order moments by the amplification factor $(1 - f_a / F'_e)$. For unbraced frame members, they are taken as 0.85. For braced frame members without transverse loading between their ends, they are computed from $C_m = 0.6 - 0.4(M_1 / M_2)$, where M_1 / M_2 is the ratio of smaller end moment to the larger end moment. For braced frame members having transverse loading between their ends, they are determined from the formula $C_m = 1 + \psi(f_a / F'_e)$ based on a rational approximate analysis outlined in AISC-ASD [22] Commentary-H1, where ψ is a parameter that considers maximum deflection and maximum moment in the member.

For the computation of allowable compression and Euler stresses, the effective length factors (K) are required. For beam and bracing members, K is taken equal to unity. For column members, alignment charts furnished in AISC-ASD [22] can be utilized. In the present work, however, the effective length factors of columns in braced and unbraced steel frames are computed from the approximate formulas (Eqs. (8), (9)) developed by Dumonteil [24], which are accurate to within about –1.0 and +2.0 % of the exact results [25]:

For unbraced members:

$$K = \sqrt{\frac{1.6G_AG_B + 4(G_A + G_B) + 7.5}{G_A + G_B + 7.5}} . \quad (8)$$

For braced members:

$$K = \frac{3G_AG_B + 1.4(G_A + G_B) + 0.64}{3G_AG_B + 2.0(G_A + G_B) + 1.28} , \quad (9)$$

where G_A and G_B refer to stiffness ratio or relative stiffness of a column at its two ends.

It is also required that the computed shear stresses (f_v) in members are smaller than the allowable shear stresses (F_v), as formulated in Eq. (10).

$$f_v \le F_v = 0.40C_vF_y \quad (10)$$

In Eq. (10), C_v is referred to as web shear coefficient. It is taken equal to C_v = 1.0 for rolled W-shaped members with $h / t_w \le 2.24\sqrt{E / F_y}$, where h is the clear distance between flanges, E is the elasticity modulus and t_w is the thickness of web. For all other symmetric shapes, C_v is calculated from Formulas G2-3, G2-4 and G2-5 in ANSI/AISC 360-05 [23].

Apart from stress constraints, slenderness limitations are also imposed on all members such that maximum slenderness ratio ($\lambda = KL / r$) is limited to 300 and 200 for tension and compression members, respectively. The displacement constraints are imposed such that the maximum lateral displacements are restricted to be less than H/400, and upper limit of story drift is set to be h/400, where H is the total height of the frame building and h is the height of a story.

Finally, we consider geometric constraints between beams and columns framing into each other at a common joint for practicality of an optimum solution generated. For the two beams B1 and B2 and the column shown in Fig. 1, one can write the following geometric constraints:

$$\frac{b_{fb}}{b_{fc}} - 1.0 \le 0 , \quad (11)$$

$$\frac{b'_{fb}}{(d_c - 2t_f)} - 1.0 \le 0 , \quad (12)$$

where b_{fb}, b'_{fb} and b_{fc} are the flange width of the beam B1, the beam B2 and the column, respectively, d_c is the depth of the column, and t_f is the flange width of the column. Eq. (11) ensures that the flange width of the beam

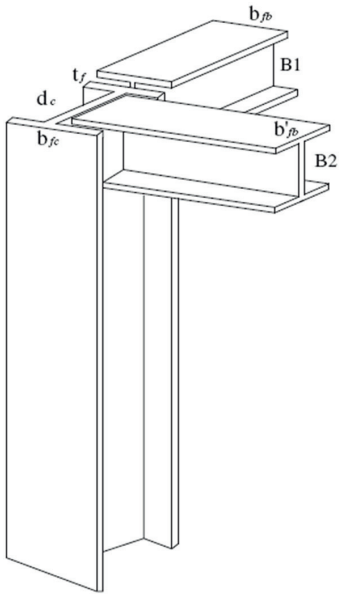

Fig. 1 Beam-column geometric constraints

B1 remains smaller than that of the column. On the other hand, Eq. (12) enables that flange width of the beam B2 remains smaller than clear distance between the flanges of the column ($d_c - 2t_f$).

3 Adaptive Dimensional Search (ADS) technique

The adaptive dimensional search (ADS) [21] is a recently proposed population-based metaheuristic optimization algorithm where only the best solution of the previous population is used to generate μ number of candidate solutions in the current population. This type of selection scheme is commonly referred to as $(1 + \mu)$-type selection in the literature and has been formerly employed by some variants of evolution strategies [26] as well as big bang-big crunch method [27].

The robustness of the ADS method lies in the idea of updating search dimensional rate (SDR) parameter online during the search to achieve a satisfactory tradeoff between exploration and exploitation features of the search process. In general, SDR can be defined as the percentage of the design variables that are perturbed probabilistically while generating a candidate solution from the current (best) design, Eq. (13)

$$\mathrm{SDR} = \frac{N_p}{N_d}, \tag{13}$$

where N_p is the number of design variables perturbed to generate a new solution and N_d is the total number of design variables. The need for changing not all, but a percentage of design variables in discrete structural optimization problems stems from the sensitivity of structural response to sizing variables in such problems. That is to say, even small changes in a few variables may yield a candidate solution that will have a completely different structural behavior than the design from which it is originated. The role of SDR parameter is to adjust explorative and exploitative search features of the ADS algorithm, which is explained in detail in the following. The steps in the implementation of the ADS can now be outlined as follows.

Step 1. Initial population: An initial population consisting of a predefined number of candidate solutions is generated randomly. This step is performed once.

Step 2. Evaluation: The population is evaluated, where structural analyses of all candidate solutions are performed with the set of steel sections selected for design variables, and force and deformation responses are obtained under the loads. The objective function values of the feasible solutions that satisfy all problem constraints are directly calculated from Eq. (2). However, infeasible solutions that violate some of the problem constraints are penalized using an external penalty function approach, and their objective function values are calculated according to Eq. (14).

$$\varphi = W\left[1 + p\left(\sum_i c_i\right)\right] \tag{14}$$

In Eq. (14), φ is the constrained objective function value, c_i is the i-th problem constraint and p is the penalty coefficient used to tune the intensity of penalization as a whole.

Step 3. Setting ADS parameter: For the initial population, the SDR parameter is set to its initial value SDR(0), which is taken as 0.25 for all the numerical examples discussed here. For other populations it is generated in the course of optimization using Eq. (15) depending on whether or not the best solution has been improved in the previous iteration $(t - 1)$ of the algorithm.

$$\mathrm{SDR}^{(t)} = \begin{cases} \dfrac{\mathrm{SDR}^{(t-1)}}{\lambda} & \textit{if the best solution is improved} \\ \lambda \cdot \mathrm{SDR}^{(t-1)} & \textit{if the best solution is not improved} \end{cases} \tag{15}$$

According to Eq. (15) if the best solution found so far is improved in the previous iteration $t - 1$, then the value of SDR is increased in the current iteration t by dividing its value by a factor $\lambda < 1.0$, otherwise SDR is decreased by multiplying its value by λ. The factor λ is referred to as search dimensional adaptation parameter (taken as 0.98 in this study), and determines the rate of adaptation towards the new value of SDR parameter. The high values of SDR motivate a more explorative search by enabling

moves in the search space through the change of many design variables at a time, resulting in large, yet relatively unfettered step sizes. On the other hand, the low values of SDR lead to a more explorative search by facilitating small, yet more conservative moves in the design space. The rationale behind Eq. (15) is to promote a more explorative search, if any of the moves in the previous iteration leads to an improved solution. This way the search dimension is increased, and the algorithm is encouraged to discover new solutions in an extended region of the search space. On the other hand, if the previous iteration leads to no improvement, diverse search is somewhat limited, and the algorithm is biased towards sampling by small and judicious moves around the current design. This way the SDR parameter is updated at each iteration to benefit from a more explorative or exploitative search alternately for the most efficient optimization process. It is recommended to define an upper and a lower bound for the variation of SDR, which are set to 0.5 and $1/N_d$, respectively where N_d refers to the total number of design variables of the optimization problem.

Step 4. New population: A new population is formed where candidate solutions are generated from the best design obtained so far using Eq. (16).

$$I_i^{new} = \begin{cases} I_i^c & \text{if } r_i > \text{SDR} \\ I_i^c + round\left[N_i(0,1)\left(\sqrt{(I_i^{\max} - I_i^{\min})} - \left(\sqrt{(I_i^{\max} - I_i^{\min})} - 1\right)\frac{t}{\max\_t}\right)\right] & \text{if } r_i \le \text{SDR} \end{cases} \quad (16)$$

In Eq. (16) I_i^c is the value of i-th design variable in the best design obtained so far, I_i^{new} is the value of the corresponding design variable in a candidate solution, and r_i is a uniform random number sampled between 0 and 1 for i-th design variable. Accordingly, while generating a candidate solution, a random number r_i is sampled anew for each design variable i. If it is greater than SDR, then the value of the i-th design variable in a candidate solution is directly copied from the best design, i.e., $I_i^{new} = I_i^c$. Otherwise ($r_i \le$ SDR); a new value is assigned to the candidate solution for the respective design variable between its lower ($I_i^{\min}$) and upper ($I_i^{\max}$) bounds using the lower expression in Eq. (16). In this expression $N_i(0,1)$ is a random number generated anew for each i-th design variable according to a standard normal distribution with mean zero and standard deviation one, t is the current iteration number, and max_t is the maximum number of iterations to be performed during the course of optimization. In case a selected design variable is not changed, a perturbation of +1 or –1 is implemented (with equal probability) to ensure a minimum change in the considered variable. It should be noted that Eq. (16) enables a change of different set of design variables for each candidate solution under the same SDR value.

Step 5. Elitism: The best solution found so far is kept in a separate place and involved in the population if any of the candidate solutions in the current population does not outperform it. It should be noted that the best design refers to either a feasible or infeasible solution with the minimum objective function value obtained so far in accordance with Eq. (2) or (14). In fact, this is the design which is used to originate candidate solutions using Eq. (16). Apart from the best design, the algorithm also stores the feasible best design, which corresponds to the best design achieved by the algorithm with strictly no constraint violation during the optimization process.

Step 6. Stagnation-control: The algorithm is checked against stagnation. Three alternative stagnation-control strategies were proposed in Hasançebi and Kazemzadeh Azad [21] for the ADS algorithm to protect it against entrapment in local optima, and thus to perform a more efficient search in the solution space. The details of different stagnation-control strategies can be found in Hasançebi and Kazemzadeh Azad [21] and are not repeated here.

Step 7. Termination: The algorithm proceeds back to Step 2 until a stopping criterion is met. This can be considered as a maximum number of iterations or no improvement of the best solution found over a certain number of iterations.

4 Design examples

In Section 4, performance evaluation of the ADS algorithm is carried out using a test set of five practical frame optimization problems. The objective in these test instances is to evaluate the performance of the ADS algorithm against several robust contemporary metaheuristics. The parameters of ADS algorithm are selected as follows. The initial value of penalty coefficient p is set to 1.0, and a population size of 50 is employed for all the examples. The annealing strategy [21] is employed for stagnation-control of the ADS algorithm, for which a limited non-improving move is permitted when a stagnation state is detected in the course of optimization.

4.1 Example 1: 132-member unbraced steel frame

The first test example shown in Fig. 2 is an unbraced space steel frame composed of 70 joints and 132 members which are grouped into 30 independent sizing variables

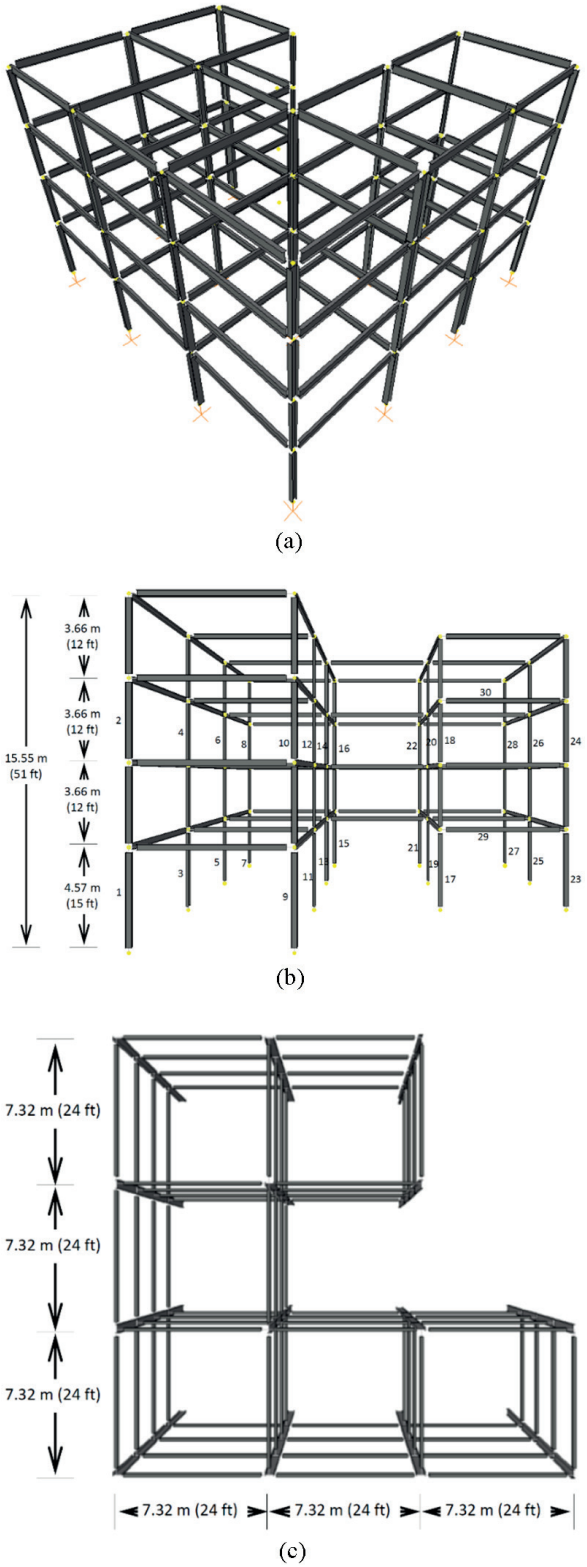

Fig. 2 132-member steel frame: (a) 3D view, (b) front view, (c) top view

(Fig. 2(b)) to satisfy practical fabrication requirements. This design optimization example has been already studied by Hasançebi et al. [28] as well as Hasançebi and Kazemzadeh Azad [29] using different optimization algorithms. Here, the columns are chosen from the complete W-shape profile list of 297 ready sections, whereas a discrete set of 171 economical sections, selected from W-shape profile list based on cross sectional area and moment of inertia properties, is used to size the beam members. Moreover, both gravity and lateral loads are considered for designing the structure. Gravity loads (G) consisting dead, live and snow loads are computed according to ASCE 7-05 [30] based on the following design values: a design dead load of 60.13 lb/ft^2 (2.88 kN/m^2), a design live load of 50 lb/ft^2 (2.39 kN/m^2), and a ground snow load of 25 lb/ft^2 (1.20 kN/m^2). This yields the uniformly distributed loads on the outer and inner beams of the roof and floors given in Table 1. As for the lateral forces, earthquake loads (E) are considered. These loads are calculated using the equivalent lateral force procedure outlined in ASCE 7-05 [30], resulting in the values given in Table 1 that are applied at the center of gravity of each story as joint loads. Gravity (G) and earthquake (E) loads are combined under two loading conditions for the frame: (i) 1.0 G + 1.0 E (in x-direction), and (ii) 1.0 G + 1.0 E (in y-direction). The combined stress, stability and geometric constraints are imposed as already explained. The joint displacements in x and y directions are limited to 1.53 in (3.59 cm) which is obtained as height of frame/400. Furthermore, story drift constraints are applied to each story of the steel frame which is equal to height of each story/400.

Discrete sizing of the 132-member steel frame is performed using the ADS algorithm and the results obtained are compared to the previously reported designs using different metaheuristic techniques in Hasançebi et al. [28], and Hasançebi and Kazemzadeh Azad [29]; namely improved simulated annealing (ISA), tabu search (TS), harmony search (HS), big bang-big crunch (BB-BC), exponential BB–BC (EBB–BC), and modified BB–BC (MBB–BC) algorithms. As presented in Table 2 the ADS algorithm produces a design weight of 125240.17 lb (56807.99 kg) for the 132-member steel frame which is the best solution of this problem reported so far. Relatively higher design weights have been obtained for the frame with other metaheuristic algorithms; namely 138874.67 lb (62993.55 kg) by ISA, 142710.96 lb (64733.69 kg) by TS, 143135.29 lb (64926.17 kg) by HS, 192834.39 lb (87468.21 kg) by BB-BC, 134050.55 lb (60804.31 kg) by EBB-BC, and 139016.28 lb (63056.72 kg) by MBB-BC. The convergence history for the best feasible design found in the course of optimization using the ADS algorithm is depicted Fig. 3.

Table 1 The gravity and lateral loading on 132-member steel frame

Gravity Loads				
Beam Type	Uniformly Distributed Load			
	Outer Span Beams		Inner Span Beams	
	(lb/ft)	(kN/m)	(lb/ft)	(kN/m)
Roof beams (Dead + Snow Loads)	1011.74	14.77	1193.84	17.42
Floor beams (Dead + Live Loads)	1468.40	21.49	1732.70	25.29
Lateral Loads				
Floor Number	Earthquake Design Load			
	(kips)		(kN)	
1	6.57		29.23	
2	12.43		55.28	
3	18.52		82.35	
4	24.76		110.15	

Table 2 Comparison of results for 132-member steel frame

Member Group	ISA	TS	HS	BB-BC	EBB-BC	MBB-BC	ADS
1	W8X35	W8X31	W14X53	W24X176	W10X33	W12X58	W8X31
2	W18X86	W12X65	W12X120	W21X132	W12X79	W14X109	W21X101
3	W12X79	W27X129	W30X48	W27X336	W40X167	W10X100	W24X104
4	W18X65	W8X58	W16X77	W24X279	W12X65	W10X54	W12X65
5	W12X65	W12X79	W18X119	W14X193	W14X120	W12X96	W24X104
6	W27X161	W12X106	W24X104	W14X109	W14X109	W14X90	W21X101
7	W24X117	W18X97	W30X148	W12X87	W14X99	W36X182	W21X101
8	W10X54	W8X58	W10X68	W27X94	W14X90	W12X65	W21X68
9	W18X86	W12X72	W18X158	W30X292	W10X100	W18X130	W12X72
10	W12X96	W14X90	W12X120	W18X283	W12X106	W14X90	W33X130
11	W10X60	W36X135	W36X150	W10X49	W33X152	W12X58	W21X68
12	W10X49	W10X49	W16X67	W21X62	W12X53	W30X99	W10X49
13	W12X87	W12X96	W10X112	W18X311	W14X90	W44X224	W14X90
14	W12X50	W10X49	W24X117	W33X141	W36X160	W40X192	W24X68
15	W24X55	W24X55	W18X40	W18X40	W18X40	W16X40	W21X44
16	W24X55	W10X33	W14X61	W12X210	W12X53	W8X35	W8X24
17	W12X58	W18X76	W12X65	W16X67	W21X111	W12X65	W14X109
18	W12X67	W21X83	W18X119	W12X65	W12X65	W12X96	W12X65
19	W12X40	W8X40	W14X82	W14X211	W14X43	W12X65	W14X43
20	W10X49	W14X61	W18X86	W14X211	W10X60	W12X65	W16X67
21	W12X72	W18X76	W14X90	W40X277	W12X106	W12X72	W10X77
22	W12X79	W12X72	W18X97	W33X141	W10X88	W12X72	W12X72
23	W8X48	W12X40	W21X73	W12X65	W8X48	W14X43	W10X49
24	W24X68	W24X76	W12X87	W30X326	W27X84	W18X119	W12X79
25	W14X61	W10X77	W18X71	W12X72	W14X61	W12X152	W10X54
26	W21X50	W16X50	W27X102	W8X28	W10X39	W12X53	W12X58
27	W8X40	W10X49	W8X48	W30X124	W12X40	W12X45	W10X39
28	W8X67	W14X61	W24X117	W24X94	W18X76	W12X72	W24X117
29	W10X39	W18X97	W18X97	W16X89	W24X68	W12X58	W12X65
30	W21X44	W16X45	W16X40	W21X44	W18X40	W16X40	W18X35
Weight, lb (kg)	138874.67 (62993.55)	142710.96 (64733.69)	143135.29 (64926.17)	192834.39 (87468.21)	134050.55 (60804.31)	139016.28 (63056.72)	125240.17 (56807.99)

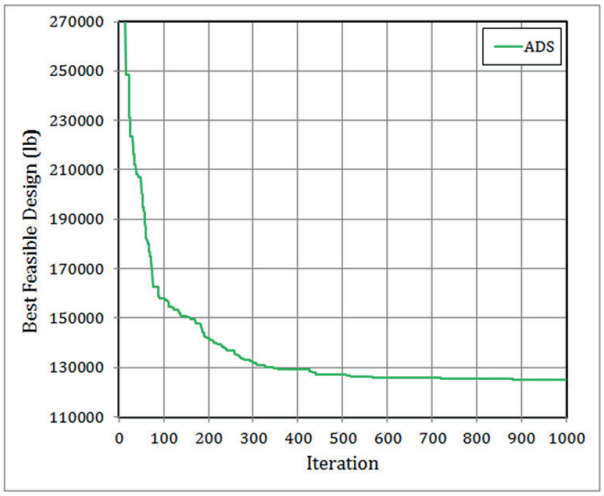

Fig. 3 Optimization history for 132-member steel frame using ADS

4.2 Example 2: 325-member braced steel frame

The space steel frame depicted in Fig. 4 is selected as the second design example for performance evaluation of the ADS algorithm. This instance has been formerly investigated in Hasançebi et al. [31]. The frame is braced with K-type bracing in the first and last bays along the x-direction and with X-type bracing system along y-direction. The 325 members of the frame are collected in 20 member groups as shown in Fig. 4(e). For this test example, gravity loads on the beams of roof and floors are tabulated in Table 3. As for lateral forces, earthquake loads (E) are computed based on the equivalent lateral force procedure outlined in ASCE 7-05 [30], resulting in point loads applied at the center of gravity of each respective story, as follows: 4.72 kips (20.99 kN) at the 1st story, 8.96 kips (39.87 kN) at the 2nd story, 13.49 kips (59.99 kN) at the 3rd story, 18.22 kips (81.04 kN) at the 4th story, and 23.11 kips (102.81 kN) at the 5th story. The gravity and lateral loads are combined under two loading conditions for the frame: (i) 1.0G + 1.0E (in x-direction), and (ii) 1.0G + 1.0E (in y-direction). As already explained, the combined stress, stability, displacement and geometric constraints are imposed according to the provisions of AISC-ASD [22].

Optimization of the 325-member braced steel frame is performed using the ADS algorithm and the results obtained as well as sectional designations for member groups are presented and compared to the results of other metaheuristics reported in Hasançebi et al. [31]. As can be seen from Table 4 the ADS algorithm locates the minimum weight as 128320.45 lb (58205.177 kg), which is the lightest of all the final designs. For this test example, relatively higher design

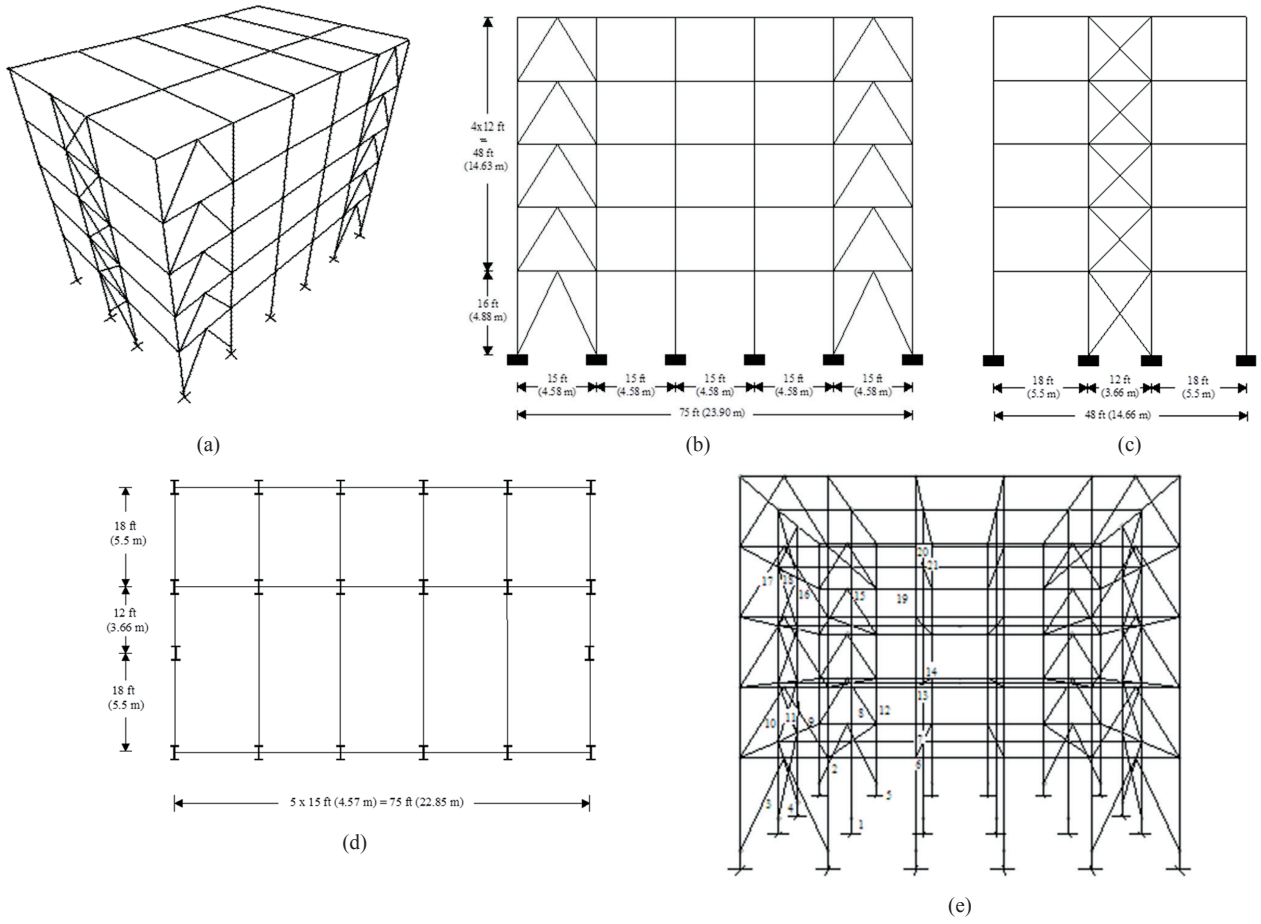

Fig. 4 325-member braced steel frame: (a) 3D view, (b) front view, (c) side view, (d) plan view, (e) member grouping

Table 3 Gravity loading on the beams of 325-member braced steel frame

Story	Beams	Uniformly Distributed Load (lb/ft)	Uniformly Distributed Load (kN/m)
Beams along y-axis			
Roof	A1-B1, A6-B6	521.67	7.61
	A2-B2, A3-B3, A4-B4, A5-B5	1043.34	15.23
	B1-C1, B6-C6	437.36	6.38
	B2-C2, B3-C3, B4-C4, B5-C5	874.72	12.77
Floor	A1-B1, A6-B6	757.14	11.05
	A2-B2, A3-B3, A4-B4, A5-B5	1514.28	22.10
	B1-C1, B6-C6	634.99	9.27
	B2-C2, B3-C3, B4-C4, B5-C5	1269.98	18.53
Beams along x-axis			
Roof	A1-A6, C1-C6	379.40	5.54
	B1-B6	758.80	11.07
Floor	A1-A6, C1-C6	550.00	8.03
	B1-B6	1101.30	16.07

weights have been found with other metaheuristic algorithms; namely 128637.77 lb (58349.11 kg) by ES, 128788.82 lb (58417.63 kg) by SA, 131782.50 lb (59775.54 kg) by TS, 133330.09 lb (60477.51 kg) by ACO, 135185.87 lb (61319.28 kg) by PSO, 138830.09 lb (62972.27 kg) by HS, and 141846.24 lb (64340.37 kg) by SGA. The convergence curve for the best feasible design obtained in the course of optimization using the ADS algorithm is plotted in Fig. 5.

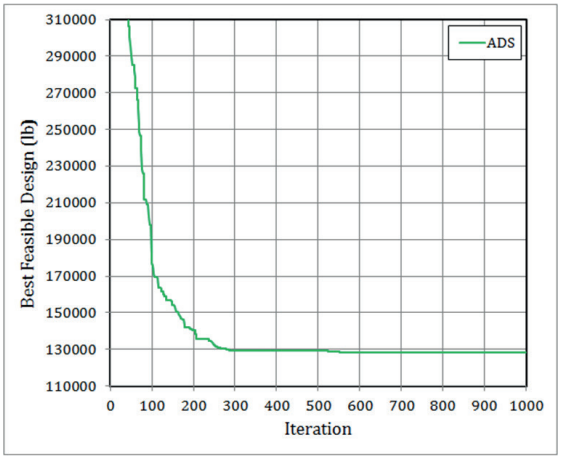

Fig. 5 Optimization history for 325-member braced steel frame using ADS

Table 4 Comparison of results for 325-member braced steel frame

Member Group	ES	SA	TS	ACO	PSO	HS	SGA	ADS
1	W8X40	W18X40	W12X35	W16X57	W18X55	W18X60	W12X30	W16X45
2	W8X24	W8X24	W8X24	W6X25	W16X40	W12X50	W18X40	W16X40
3	W21X62	W18X60	W12X53	W21X68	W14X61	W14X61	W24X68	W10X26
4	W6X15	W6X15	W6X20	W6X15	W6X15	W8X18	W5X19	W18X60
5	W18X50	W16X45	W18X50	W8X40	W12X40	W16X45	W14X43	W12X14
6	W12X14	W12X14	W10X17	W12X14	W12X16	W10X15	W10X19	W18X40
7	W18X40	W18X40	W18X40	W21X44	W21X44	W18X40	W18X46	W6X15
8	W8X18	W8X24	W8X21	W8X24	W8X18	W16X31	W10X26	W21X44
9	W8X18	W14X22	W6X15	W8X21	W10X22	W14X30	W14X22	W8X21
10	W12X50	W12X50	W14X53	W14X48	W16X50	W12X53	W12X50	W10X19
11	W6X15	W6X15	W6X15	W6X15	W6X15	W6X15	W6X20	W12X50
12	W21X44	W21X44	W18X46	W16X50	W8X48	W12X50	W18X46	W12X14
13	W12X14	W12X14	W12X16	W12X14	W12X44	W12X16	W12X19	W18X40
14	W18X40	W18X40	W18X40	W18X40	W21X44	W18X40	W18X40	W6X15
15	W8X13	W8X13	W8X15	W8X15	W8X18	W8X15	W12X19	W14X34
16	W12X14	W12X14	W12X14	W12X19	W12X14	W12X16	W8X24	W8X13
17	W14X34	W14X34	W16X36	W14X34	W16X36	W10X33	W12X35	W8X13
18	W6X15	W6X15	W5X16	W6X15	W6X15	W6X15	W6X20	W14X34
19	W14X34	W14X34	W14X34	W14X34	W16X36	W12X45	W14X30	W12X14
20	W12X14	W12X14	W12X14	W12X16	W12X14	W12X14	W12X16	W18X40
21	W18X40	W18X40	W18X40	W18X40	W18X40	W18X40	W21X44	W6X15
Weight, lb (kg)	128637.77 (58349.11)	128788.82 (58417.63)	131782.50 (59775.54)	133330.09 (60477.51)	135185.87 (61319.28)	138830.09 (62972.27)	141846.24 (64340.37)	128320.45 (58205.177)

4.3 Example 3: 568-member unbraced steel frame

The third design instance is an unbraced space steel frame (Fig. 6) composed of 256 joints and 568 members which are collected in 25 member groups. This optimization example has been already studied in Hasançebi et al. [31] using various metaheuristics. The frame is subjected to two loading conditions of combined gravity and wind forces. The wind forces are calculated based on a basic wind speed of 105 mph (46.94 m/s). The resulting gravity loading on the beams of roof and floors is tabulated in Table 5 and the wind loading is given in Table 6. In the first loading condition, gravity loading is applied with wind loading acting along x-axis, whereas in the second one wind loading is acted along y-axis.

Table 5 Gravity loading on the beams of 568-member unbraced steel frame

Beam Type	Uniformly Distributed Load			
	Outer Beams		Inner Beams	
	(lb/ft)	(kN/m)	(lb/ft)	(kN/m)
Roof beams	505.88	7.38	1011.74	14.77
Floor beams	734.20	10.72	1468.40	21.44

Optimization of the 568-member unbraced steel frame is carried out using the ADS algorithm and the results achieved as well as sectional designations for member groups are presented and compared to the results of other metaheuristics reported in Hasançebi et al. [31]. As can be seen from Table 7 the ADS algorithm finds a promising solution

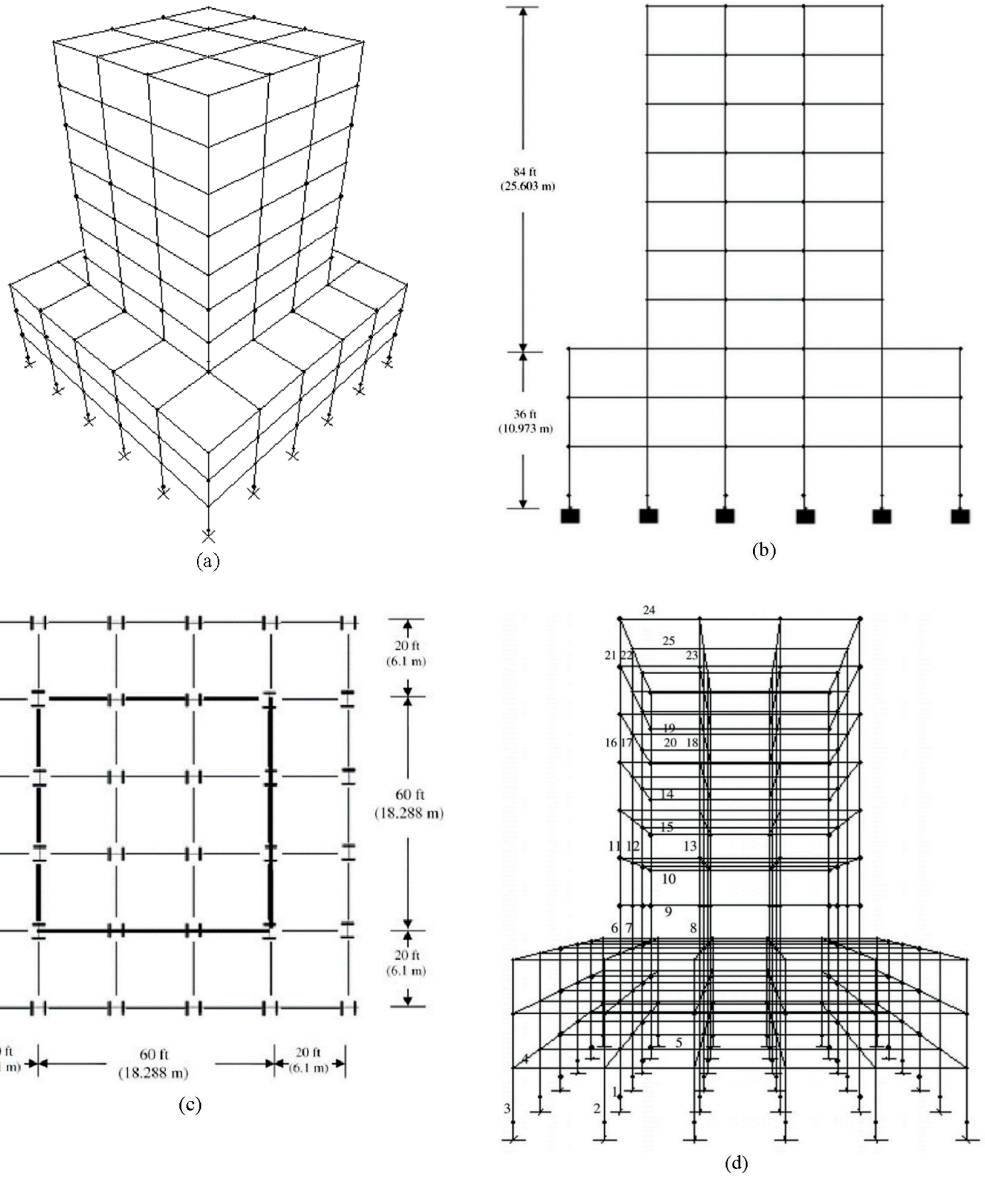

Fig. 6 568-member unbraced steel frame: (a) 3D view, (b) elevation view, (c) plan view, (d) member grouping

Table 6 Wind loading on 568-member unbraced steel frame

Floor No	Windward		Leeward	
	(lb/ft)	(kN/m)	(lb/ft)	(kN/m)
1	112.51	1.64	127.38	1.86
2	128.68	1.88	127.38	1.86
3	144.68	2.10	127.38	1.86
4	156.86	2.29	127.38	1.86
5	167.19	2.44	127.38	1.86
6	176.13	2.57	127.38	1.86
7	184.06	2.69	127.38	1.86
8	191.21	2.79	127.38	1.86
9	197.76	2.89	127.38	1.86
10	101.90	1.49	63.90	1.86

with a design weight of 505781.22 lb (229418.50 kg) which is slightly heavier than the best solution found by ES, i.e. 503953.63 lb (228588.33 kg). Here, relatively higher design weights have been obtained using other meta-heuristic algorithms; namely 526370.76 lb (238756.51 kg) by SA, 518458.35 lb (235167.52 kg) by TS, 532353.70 lb (241470.31 kg) by ACO, 558346.15 lb (253260.23 kg) by PSO, 571159.66 lb (259072.31 kg) by HS, and 541380.54 lb (245564.80 kg) by SGA. The convergence curve for the best feasible design obtained in the course of optimization using the ADS algorithm is depicted in Fig. 7.

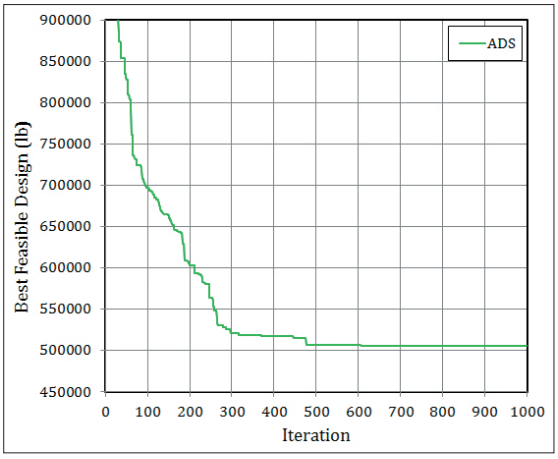

Fig. 7 Optimization history for 568-member unbraced steel frame using ADS

Table 7 Comparison of results for 568-member unbraced steel frame

Member Group	ES	TS	SA	ACO	SGA	PSO	HS	ADS
1	W14X193	W14X193	W14X193	W14X193	W14X193	W14X159	W14X176	W14X193
2	W8X48	W8X48	W8X48	W8X48	W8X48	W24X76	W12X53	W10X45
3	W10X39	W8X40	W8X40	W10X45	W10X39	W10X39	W8X40	W8X48
4	W10X22	W10X22	W10X22	W10X22	W10X26	W10X22	W10X22	W10X22
5	W21X50	W21X50	W21X44	W21X50	W21X50	W24X55	W24X55	W21X50
6	W10X54	W10X54	W12X65	W14X61	W18X76	W12X72	W24X117	W12X58
7	W14X109	W14X120	W14X145	W14X120	W14X109	W27X146	W24X146	W14X109
8	W14X176	W14X159	W14X145	W40X192	W40X192	W27X217	W40X199	W14X159
9	W18X40	W21X44	W24X68	W18X35	W18X40	W18X40	W21X44	W18X35
10	W18X40	W18X40	W24X55	W18X40	W21X50	W18X40	W18X40	W21X50
11	W10X49	W10X45	W10X49	W12X58	W12X65	W18X71	W27X94	W10X49
12	W14X90	W14X90	W14X90	W12X96	W21X111	W21X101	W14X120	W14X90
13	W14X109	W12X120	W14X120	W12X136	W12X152	W14X176	W14X120	W14X120
14	W14X30	W21X44	W16X36	W12X30	W12X30	W14X34	W12X30	W14X30
15	W16X36	W16X36	W16X40	W21X44	W16X40	W21X44	W18X40	W16X36
16	W12X45	W10X33	W12X40	W8X58	W14X68	W12X65	W27X94	W8X48
17	W12X65	W12X65	W12X65	W18X76	W18X76	W10X68	W18X97	W12X65
18	W10X22	W14X34	W12X26	W12X35	W8X28	W12X35	W12X30	W10X22
19	W12X79	W12X79	W12X72	W10X88	W10X88	W12X79	W10X88	W12X79
20	W14X30	W14X30	W16X36	W14X30	W16X36	W14X38	W18X35	W14X30
21	W8X35	W10X39	W8X24	W8X58	W8X48	W10X39	W12X72	W8X35
22	W10X39	W12X45	W10X49	W8X40	W14X34	W8X31	W10X45	W16X40
23	W8X31	W12X35	W8X24	W8X31	W12X30	W12X96	W14X132	W10X49
24	W8X18	W6X20	W12X26	W8X24	W8X21	W12X26	W18X35	W8X18
25	W14X30	W12X26	W12X26	W16X45	W18X35	W12X26	W16X36	W12X26
Weight, lb (kg)	503953.63 (228588.33)	518458.35 (235167.52)	526370.76 (238756.51)	532353.70 (241470.31)	541380.54 (245564.80)	558346.15 (253260.23)	571159.66 (259072.31)	505781.22 (229418.50)

4.4 Example 4: 744-member unbraced steel frame

The fourth design optimization instance is an unbraced space steel frame composed of 315 joints and 744 structural members which are collected in 16 different member groups. Fig. 8 depicts the side, plan, and 3D views of the frame as well as the corresponding member grouping details. This test example has been formerly investigated in Hasançebi et al. [32]. The frame is subjected to two loading conditions of combined gravity and wind forces as follows. The uniformly distributed gravity loads of 379.4 lb/ft (5.54 kN/m) and 758.8 lb/ft (11.08 kN/m) are applied on the exterior and interior top story beams, respectively, whereas exterior and interior beams of the other floors are subjected to uniformly distributed gravity loads of 550.65 lb/ft (8.04 kN/m) and 1101.3 lb/ft (16.08 kN/m), respectively. Here, the design wind speed is taken as 121 mph (54.09 m/s) and the corresponding lateral (wind) loads acting at each floor level on windward and leeward faces of the frame are presented in Table 8. In the first loading case, the gravity loads are applied together with the wind loads acting along the x-axis, whereas in the second case they are applied together with the wind loads acting along the y-axis. The combined stress, stability, displacement and geometric constraints are imposed according to the provisions of AISC-ASD [22], as given in Section 2.

Discrete sizing optimization of the 744-member steel frame is performed using the ADS algorithm and the obtained results are compared to the previously reported designs in Hasançebi et al. [32] using different metaheuristic techniques, namely standard harmony search (HS),

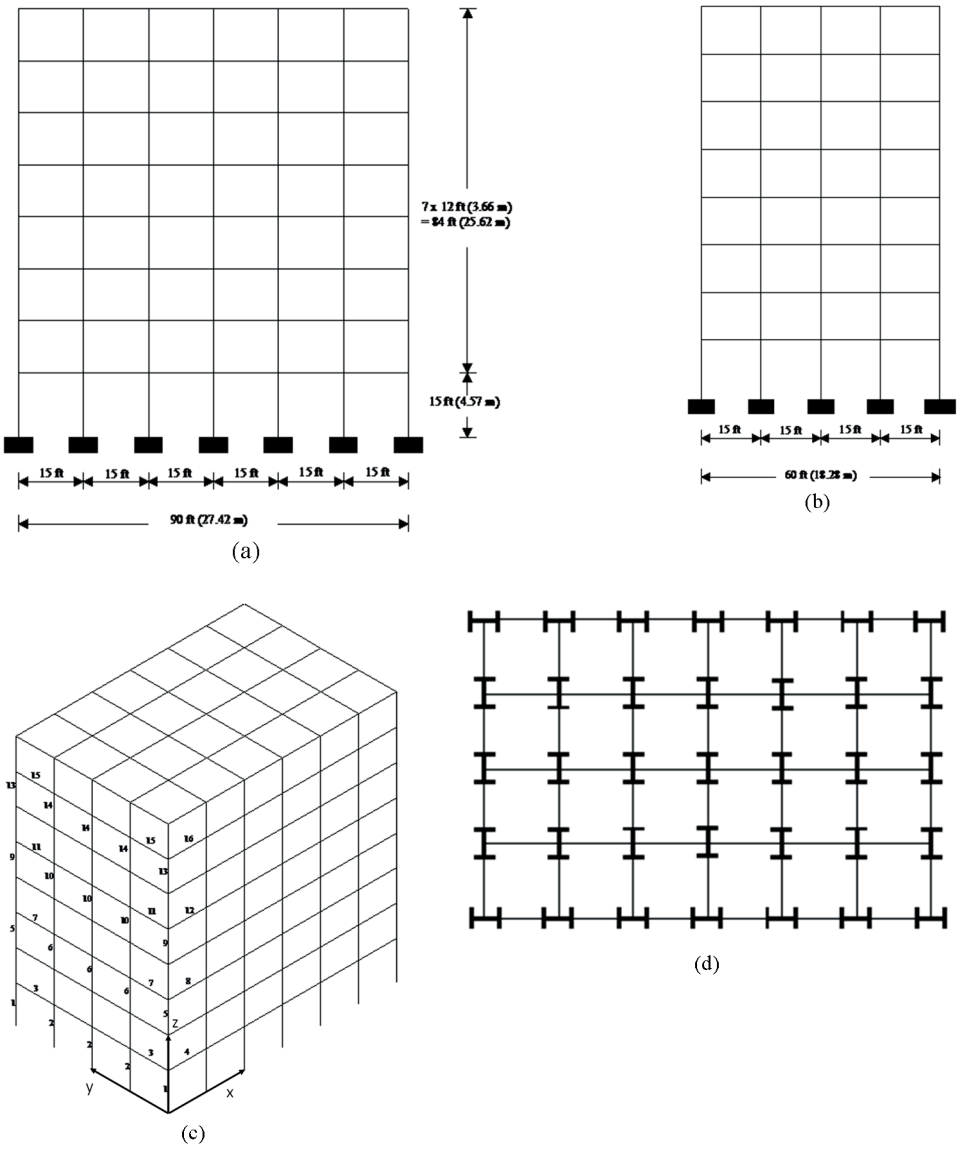

Fig. 8 744-member unbraced steel frame: (a) side view (x-z plane), (b) side view (y-z plane), (c) 3D view, (d) plan view

Table 8 Wind forces on 744-member unbraced steel frame

Floor No	Windward		Leeward	
	(lb/ft)	(kN/m)	(lb/ft)	(kN/m)
1	140.64	0.63	159.22	0.71
2	171.44	0.76	159.22	0.71
3	192.49	0.86	159.22	0.71
4	208.98	0.93	159.22	0.71
5	222.74	0.99	159.22	0.71
6	234.65	1.04	159.22	0.71
7	245.22	1.09	159.22	0.71
8	127.38	0.57	79.61	0.36

adaptive harmony search (AHS), tabu search (TS), ant colony optimization (ACO), particle swarm optimization (PSO), and simple genetic algorithm (SGA). As tabulated in Table 9, the ADS algorithm produces a design weight of 399650.79 lb (181281.56 kg) which is slightly heavier than the best solution found by AHS, i.e. 395708.03 lb (179493.16 kg). For this test example, relatively higher design weights have been achieved using other meta-heuristic techniques; namely 420177.57 lb (190592.55 kg) by HS, 401647.84 lb (182136.90 kg) by TS, 405441.65 lb (183908.33 kg) by ACO, 412200.98 lb (186974.36 kg) by PSO, and 424076.52 lb (192361.11 kg) by SGA.

4.5 Example 5: 1860-member braced steel frame

The last design example investigated in the present study is a 36-story braced steel frame composed of 814 joints and 1860 structural members. This design optimization instance has been formerly studied in Hasançebi and Kazemzadeh Azad [33] as well as Saka and Hasançebi [34] using meta-heuristic techniques. The side, top and 3D views of the frame as well as member grouping details are shown in Fig. 9. An economical and effective stiffening of the frame against lateral forces is achieved through exterior diagonal bracing members located on the perimeter of the building, which also participate in transmitting the gravity forces.

The wide-flange (W) profile list consisting of 297 ready sections is used to size the column members, while beams and diagonals are taken from discrete sets of 171 and 147 economical sections selected from wide-flange profile list based on cross sectional area and moment of inertia properties in the former, and on area and radius of gyration properties in the latter. The 1860 frame members are collected in 72 different member groups, considering the symmetry of the structure and practical fabrication requirements. That is, the columns in a story are collected in three member groups as corner columns, inner columns and outer columns, whereas beams are divided into two

Table 9 Comparison of results for 744-member unbraced steel frame

Member Group	AHS	HS	TS	ACO	PSO	SGA	ADS
1	W12X87	W12X79	W8X35	W12X72	W14X99	W24X68	W12X79
2	W14X109	W14X132	W14X145	W14X109	W14X99	W14X120	W14X109
3	W10X22	W14X22	W16X26	W14X22	W8X18	W8X21	W14X22
4	W18X35	W16X36	W18X35	W18X40	W21X44	W21X44	W18X40
5	W12X65	W12X72	W8X24	W10X49	W14X48	W12X65	W10X54
6	W12X79	W12X87	W14X90	W12X87	W14X90	W12X79	W12X79
7	W10X22	W14X22	W14X22	W12X26	W16X31	W14X26	W14X22
8	W16X26	W16X26	W18X35	W16X26	W14X26	W16X26	W16X31
9	W8X31	W16X40	W10X54	W12X35	W8X31	W8X35	W14X43
10	W12X65	W12X65	W12X53	W12X72	W14X90	W12X72	W12X72
11	W14X22	W14X22	W6X20	W14X22	W8X18	W14X26	W8X18
12	W14X22	W16X26	W16X26	W16X26	W16X26	W14X22	W14X22
13	W6X20	W16X36	W8X24	W10X39	W8X31	W8X35	W12X26
14	W12X58	W8X35	W8X40	W8X35	W8X31	W8X35	W10X45
15	W8X18	W10X22	W8X18	W8X21	W8X18	W8X21	W8X18
16	W14X22	W14X22	W14X26	W10X22	W14X22	W18X35	W14X22
Weight, lb (kg)	395708.03 (179493.16)	420177.57 (190592.55)	401647.84 (182136.90)	405441.65 (183908.33)	412200.98 (186974.36)	424076.52 (192361.11)	399650.79 (181281.56)

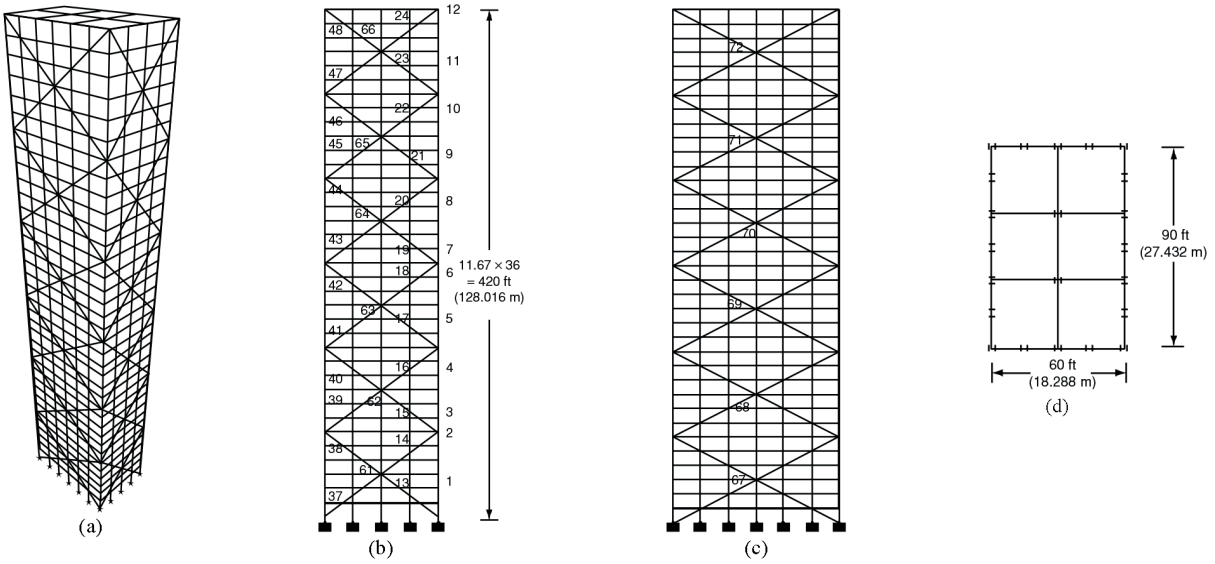

Fig. 9 Schematic of the spatial 1860-member braced, (a) 3-D view, (b) front view and member grouping, (c) side view, (d) top view

groups as inner beams and outer beams. The corner columns are grouped together as having the same section over three adjacent stories, as are inner columns, outer columns, inner beams and outer beams. Bracing members on each facade are designed as three-story deep members, and two bracing groups are specified at every six stories.

The 1860-member braced space steel frame is subjected to two loading conditions of combined gravity and wind forces. These forces are computed as per ASCE 7-05 [30] based on the following design values: a design dead load of 2.88 kN/m^2 (60.13 lb/ft^2), a design live load of 2.39 kN/m^2 (50 lb/ft^2), a ground snow load of 1.20 kN/m^2 (25 lb/ft^2) and a basic wind speed of 55.21 m/s (123.5 mph). Lateral (wind) loads acting at each floor level on windward and leeward faces of the frame are tabulated in Table 10 and the gravity loading on the beams of roof and floors is given in Table 11. In the first loading condition, gravity loads are applied together with wind loads acting along x-axis (1.0 GL + 1.0 WL-x), whereas in the second loading condition they are applied with wind loads acting along y-axis (1.0 GL + 1.0vWL-y). The joint displacements in x and y-directions are restricted to 32.0 cm (12.6 in) which corresponds to 1/400 of the frame height. Moreover, story drift constraints are imposed at each story of the frame which is equal to 1/400 of story height.

Optimal sizing of the 1860-member braced steel frame is carried out using the ADS algorithm and the results are compared to the previously reported designs in the literature using the bat-Inspired (BI) [33] and AHS [34] algorithms. As given in Table 12, the ADS algorithm obtains a promising design weight of 4858.33 kips (2203.7 tons) which is slightly heavier than the best solution found by BI algorithm, i.e. 4822.6 kips (2187.5 tons). For this design optimization example, a relatively higher design weight of 5254.9 kips (2383.6 tons) has been achieved using AHS algorithm.

It is worth mentioning that, although in this study the application of the ADS algorithm is limited to single-objective optimization problems, it is possible to reformulate the algorithm to handle multi-objective optimization instances as well. Moreover, akin to other metaheuristics, the ADS algorithm does not guarantee the convergence to a global optimum. However, as shown in the present study, comparison of the performance of the ADS versus other contemporary metaheuristics clearly indicates the efficiency of this technique in optimum design of real size steel frames. Finally, it should be noted that the conclusions drawn in this study are valid for the investigated test examples only and may not be valid for the cases not investigated here.

5 Conclusions

In this study, a recently developed metaheuristic optimization algorithm, namely adaptive dimensional search technique, is applied to discrete sizing optimization of real-size steel frames. Beside the simple algorithmic structure and efficiency of the algorithm, an important feature of the ADS is that its working principles are not based on any metaphor. Instead, the algorithm uses an efficient performance-oriented methodology for searching the optimum in the design space. The performance of the ADS is investigated using five practical instances of steel frames and the obtained results are compared to those of several metaheuristic techniques available in the literature.

The comparison of the numerical results indicates that the ADS algorithm can be efficiently employed for sizing optimization of steel frames under realistic design constraints. There is scope for further research to reformulate the ADS algorithm for handling multi-objective optimization problems as well as other engineering design instances such as optimum design of reinforced concrete frames or other composite structural systems.

Table 10 Wind loads acting on the spatial 1860-member braced steel frame

Floor	Windward kN/m (lb/ft)	LeewardkN/m (lb/ft)
1	2.05 (140.64)	3.57 (244.70)
2	2.50 (171.44)	3.57 (244.70)
3	2.81 (192.49)	3.57 (244.70)
4	3.05 (208.98)	3.57 (244.70)
5	3.25 (222.74)	3.57 (244.70)
6	3.42 (234.65)	3.57 (244.70)
7	3.58 (245.22)	3.57 (244.70)
8	3.72 (254.75)	3.57 (244.70)
9	3.85 (263.47)	3.57 (244.70)
10	3.96 (271.52)	3.57 (244.70)
11	4.07 (279.02)	3.57 (244.70)
12	4.18 (286.04)	3.57 (244.70)
13	4.27 (292.66)	3.57 (244.70)
14	4.36 (298.92)	3.57 (244.70)
15	4.45 (304.87)	3.57 (244.70)
16	4.53 (310.55)	3.57 (244.70)
17	4.61 (315.97)	3.57 (244.70)
18	4.69 (321.18)	3.57 (244.70)
19	4.76 (326.18)	3.57 (244.70)
20	4.83 (330.99)	3.57 (244.70)
21	4.90 (335.64)	3.57 (244.70)
22	4.97 (340.13)	3.57 (244.70)
23	5.03 (344.48)	3.57 (244.70)
24	5.09 (348.69)	3.57 (244.70)
25	5.15 (352.78)	3.57 (244.70)
26	5.21 (356.76)	3.57 (244.70)
27	5.27 (360.62)	3.57 (244.70)
28	5.32 (364.39)	3.57 (244.70)
29	5.37 (368.06)	3.57 (244.70)
30	5.43 (371.65)	3.57 (244.70)
31	5.48 (375.14)	3.57 (244.70)
32	5.53 (378.56)	3.57 (244.70)
33	5.58 (381.90)	3.57 (244.70)
34	5.62 (385.18)	3.57 (244.70)
35	5.67 (388.38)	3.57 (244.70)
36	2.86 (195.76)	1.79 (122.35)

Table 11 Gravity loads acting on the spatial 1860-member braced steel frame

Beam Type	Uniformly Distributed Load, kN/m (lb/ft)		
	Dead Load	Live Load	Snow Load
Roof beams	22.44 (1536.66)	N.A	5.88 (402.50)
Floor beams	22.44 (1536.66)	18.66 (1277.78)	N.A

Table 12 Comparison of results for 1860-member braced steel frame

Member Group	AHS Section	AHS Member Group	AHS Section	BI Member Group	BI Section	BI Member Group	BI Section	ADS Member Group	ADS Section	ADS Member Group	ADS Section
1	W24X370	37	W12X14	1	W14X398	37	W12X16	1	W14X398	37	W12X16
2	W12X336	38	W16X26	2	W40X531	38	W12X19	2	W40X531	38	W12X19
3	W12X305	39	W14X22	3	W24X306	39	W10X22	3	W24X306	39	W12X26
4	W12X190	40	W14X26	4	W18X258	40	W8X24	4	W40X244	40	W8X24
5	W14X193	41	W27X102	5	W14X109	41	W12X26	5	W14X109	41	W12X30
6	W24X117	42	W16X31	6	W27X114	42	W14X38	6	W14X145	42	W12X35
7	W12X79	43	W18X35	7	W33X152	43	W12X26	7	W33X152	43	W12X26
8	W12X79	44	W18X35	8	W24X192	44	W44X198	8	W24X192	44	W44X198
9	W40X244	45	W40X167	9	W30X116	45	W14X26	9	W30X116	45	W14X26
10	W18X86	46	W14X22	10	W24X146	46	W14X26	10	W24X146	46	W14X26
11	W12X96	47	W24X68	11	W16X40	47	W14X30	11	W16X40	47	W16X36
12	W8X28	48	W16X26	12	W12X136	48	W24X68	12	W21X122	48	W24X68
13	W33X424	49	W24X62	13	W27X448	49	W21X62	13	W27X448	49	W21X62
14	W40X436	50	W27X94	14	W24X370	50	W24X68	14	W24X370	50	W24X68
15	W40X324	51	W24X68	15	W40X324	51	W21X68	15	W40X324	51	W21X68
16	W36X280	52	W24X76	16	W27X281	52	W21X83	16	W27X307	52	W21X83
17	W33X318	53	W24X76	17	W14X233	53	W24X76	17	W40X244	53	W24X76
18	W33X291	54	W30X116	18	W33X241	54	W21X83	18	W33X241	54	W21X83
19	W40X277	55	W27X94	19	W27X235	55	W33X118	19	W27X235	55	W33X118
20	W24X250	56	W21X83	20	W36X300	56	W24X84	20	W36X300	56	W24X84
21	W36X260	57	W30X90	21	W40X244	57	W27X94	21	W27X258	57	W27X94
22	W33X291	58	W44X198	22	W14X211	58	W30X90	22	W14X211	58	W30X90
23	W27X235	59	W44X285	23	W14X159	59	W21X83	23	W14X159	59	W21X83
24	W12X170	60	W24X68	24	W14X159	60	W21X83	24	W14X159	60	W21X83
25	W14X665	61	W14X455	25	W36X848	61	W14X370	25	W36X848	61	W14X370
26	W36X798	62	W14X398	26	W36X848	62	W14X398	26	W36X848	62	W14X398
27	W36X720	63	W40X328	27	W36X848	63	W14X370	27	W36X848	63	W14X370
28	W33X619	64	W14X233	28	W36X848	64	W14X193	28	W36X848	64	W14X193
29	W40X531	65	W14X109	29	W36X848	65	W14X132	29	W36X848	65	W14X132
30	W36X439	66	W12X72	30	W36X848	66	W14X90	30	W36X848	66	W14X90
31	W27X494	67	W40X328	31	W40X655	67	W40X244	31	W40X655	67	W40X244
32	W33X619	68	W14X283	32	W27X407	68	W14X233	32	W27X407	68	W14X233
33	W21X364	69	W14X233	33	W27X368	69	W14X233	33	W36X359	69	W14X233
34	W40X297	70	W40X192	34	W30X357	70	W33X221	34	W36X328	70	W33X221
35	W36X245	71	W40X192	35	W36X232	71	W14X99	35	W36X232	71	W14X99
36	W14X283	72	W14X132	36	W27X129	72	W14X90	36	W27X129	72	W14X90
Weight, kips (tons)		5254.9 (2383.6)			4822.6 (2187.5)				4858.33 (2203.7)		

References

[1] Saka, M. P. "Optimum Design of Steel Frames using Stochastic Search Techniques Based on Natural Phenomena: A Review", In: Topping, B. H. V. (ed.) Civil Engineering Computations: Tools and Techniques, Saxe-Coburg Publications, Stirlingshire, UK, 2007, pp. 105–147. https://doi.org/10.4203/csets.16.6

[2] Saka, M. P. "Optimum design of steel frames with stability constraints", Computers & Structures, 41(6), pp. 1365–1377, 1991. https://doi.org/10.1016/0045-7949(91)90274-P

[3] Erdal, F., Dogan, E., Saka, M. P. "An improved particle swarm optimizer for steel grillage systems", Structural Engineering and Mechanics, 47(4), pp. 513–530, 2013. https://doi.org/10.12989/sem.2013.47.4.513

[4] Kaveh, A., Talatahari, S. "Hybrid Algorithm of Harmony Search, Particle Swarm and Ant Colony for Structural Design Optimization", In: Geem, Z. W. (ed.) Harmony Search Algorithms for Structural Design Optimization, Springer, Berlin, Heidelberg, Germany, 2009, pp. 159–198. https://doi.org/10.1007/978-3-642-03450-3_5

[5] Kaveh, A., Talatahari, S. "A Discrete Big Bang-Big Crunch Algorithm for Optimal Design of Skeletal Structures", Asian Journal of Civil Engineering, 11(1), pp. 103–122, 2010. [online] Available at: https://ajce.bhrc.ac.ir/Journal-Volumes-Issues/agentType/View/PropertyID/6120 [Accessed: 24 September 2019]

[6] Kaveh, A., Talatahari, S. "Optimum design of skeletal structures using imperialist competitive algorithm", Computers & Structures, 88(21–22), pp. 1220–1229, 2010. https://doi.org/10.1016/j.compstruc.2010.06.011

[7] Ozturk, H. T., Durmus, A. "Optimum cost design of RC columns using artificial bee colony algorithm", Structural Engineering and Mechanics, 45(5), pp. 643–654, 2013. https://doi.org/10.12989/sem.2013.45.5.643

[8] Erdal, F. "The comparative analysis of optimal designed web expanded beams via improved harmony search method", Structural Engineering and Mechanics, 54(4), pp. 665–691, 2015. https://doi.org/10.12989/sem.2015.54.4.665

[9] Gholizadeh, S., Gheyratmand, C., Davoudi, H. "Optimal design of double layer barrel vaults considering nonlinear behavior", Structural Engineering and Mechanics, 58(6), pp. 1109–1126, 2016. https://doi.org/10.12989/sem.2016.58.6.1109

[10] Tejani, G. G., Bhensdadia, V. H., Bureerat, S. "Examination of three meta-heuristic algorithms for optimal design of planar steel frames", Advances in Computational Design, 1(1), pp. 79–86, 2016. https://doi.org/10.12989/acd.2016.1.1.079

[11] Bhensdadia, V., Tejani, G. "Grey Wolf Optimizer (GWO) Algorithm for Minimum Weight Planer Frame Design Subjected to AISC-LRFD", Advances in Intelligent Systems and Computing, 409, pp. 143–151, 2016. https://doi.org/10.1007/978-981-10-0135-2_13

[12] Goldberg, D. E., Samtani, M. P. "Engineering Optimization Via Genetic Algorithm", In: Proceedings of the Ninth Conference on Electronic Computation, ASCE, New York, USA, 1986, pp. 471–482.

[13] Kennedy, J., Eberhart, R. "Particle swarm optimization", In: Proceedings of ICNN'95-International Conference on Neural Networks, Perth, WA, Australia, 1995, pp. 1942–1948. https://doi.org/10.1109/ICNN.1995.488968

[14] Colorni, A., Dorigo, M., Maniezzo, V. "Distributed Optimization by Ant Colonies", In: Proceedings of the first European Conference on Artificial Life, Paris, France, 1991, pp. 134–142.

[15] Dorigo, M. "Optimization, learning and natural algorithms", PhD Thesis, Politecnico di Milano, 1992.

[16] Yang, X. S. "Nature-Inspired Metaheuristic Algorithms", Luniver Press, UK, 2008.

[17] Lamberti, L., Pappalettere, C. "Metaheuristic Design Optimization of Skeletal Structures: A Review", Computational Technology Reviews, 1, pp. 1–32, 2011. https://doi.org/10.4203/ctr.4.1

[18] Koohestani, K., Kazemzadeh Azad, S. "An Adaptive Real-Coded Genetic Algorithm for Size and Shape Optimization of Truss Structures", In: Topping, B. H. V., Tsompanakis, Y. (eds.) Proceedings of the First International Conference on Soft Computing Technology in Civil, Structural and Environmental Engineering, Civil-Comp Press, Stirlingshire, UK, 2009, Paper 13. https://doi.org/10.4203/ccp.92.13

[19] Tejani, G. G., Pholdee, N., Bureerat, S., Prayogo, D. "Multiobjective adaptive symbiotic organisms search for truss optimization problems", Knowledge-Based Systems, 161, pp. 398–414, 2018. https://doi.org/10.1016/j.knosys.2018.08.005

[20] Tejani, G. G., Pholdee, N., Bureerat, S., Prayogo, D., Gandomi, A. H. "Structural optimization using multi-objective modified adaptive symbiotic organisms search", Expert Systems with Applications, 125, pp. 425–441, 2019. https://doi.org/10.1016/j.eswa.2019.01.068

[21] Hasançebi, O., Kazemzadeh Azad, S. "Adaptive dimensional search: A New metaheuristic algorithm for discrete truss sizing optimization", Computers & Structures, 154, pp. 1–16, 2015. https://doi.org/10.1016/j.compstruc.2015.03.014

[22] AISC-ASD "Manual of steel construction-allowable stress design", 9th ed., American Institute of Steel Construction, Chicago, Illinois, USA, 1989.

[23] ANSI/AISC 360-05 "Specification for structural steel buildings", American Institute of Steel Construction, Chicago, Illinois, USA, 2005.

[24] Dumonteil, P. "Simple Equations for Effective Length Factors", Engineering Journal, American Institute of Steel Construction, 29, pp. 111–115, 1992.

[25] Hellesland, J. "Review and evaluation of effective length formulas", University of Oslo, Oslo, Norway, Rep. 94–2, 1994. [online] Available at: https://www.duo.uio.no/handle/10852/10381?locale-attribute=en [Accessed: 25 September 2019]

[26] Schwefel, H. P. "Numerical optimization of computer models", John Wiley & Sons, Chichester, UK, 1981.

[27] Erol, O. K., Eksin, I. "A new optimization method: Big Bang-Big Crunch", Advances in Engineering Software, 37(2), pp. 106–111, 2006. https://doi.org/10.1016/j.advengsoft.2005.04.005

[28] Hasançebi, O., Çarbaş, S., Saka, M. P. "Improving the performance of simulated annealing in structural optimization", Structural and Multidisciplinary Optimization, 41(2), pp. 189–203, 2010. https://doi.org/10.1007/s00158-009-0418-9

[29] Hasançebi, O., Kazemzadeh Azad, S. "An exponential big bang-big crunch algorithm for discrete design optimization of steel frames", Computers & Structures, 110–111, pp. 167–179, 2012. https://doi.org/10.1016/j.compstruc.2012.07.014

[30] ASCE 7-05 "Minimum design loads for buildings and other structures", American Society of Civil Engineers, Reston, VA, USA, 2005.

[31] Hasançebi, O., Çarbas, S., Dogan, E., Erdal, F., Saka, M. P. "Comparison of non-deterministic search techniques in the optimum design of real size steel frames", Computers & Structures, 88(17–18), pp. 1033–1048, 2010. https://doi.org/10.1016/j.compstruc.2010.06.006

[32] Hasançebi, O., Erdal, F., Saka, M. P. "Adaptive Harmony Search Method for Structural Optimization", Journal of Structural Engineering, 136(4), pp. 419–431, 2010.
https://doi.org/10.1061/(ASCE)ST.1943-541X.0000128

[33] Hasançebi, O., Kazemzadeh Azad, S. "Improving Computational Efficiency of Bat-Inspired Algorithm in Optimal Structural Design", Advances in Structural Engineering, 18(7), pp. 1003–1015, 2015.
https://doi.org/10.1260/1369-4332.18.7.1003

[34] Saka, M. P., Hasançebi, O. "Adaptive Harmony Search Algorithm for Design Code Optimization of Steel Structures", In: Geem, Z. W. (ed.) Harmony Search Algorithms for Structural Design Optimization, Studies in Computational Intelligence, Springer, Berlin, Heidelberg, Germany, 2009, pp. 79–120.
https://doi.org/10.1007/978-3-642-03450-3_3